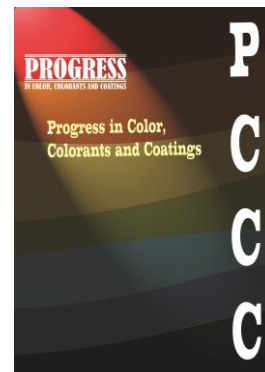


Accepted Manuscript

**Title: Enhancing Anti-Aging Properties of Golden-Phase Leaves via Zinc Oxide–PVA–Chitosan Coating**



**Authors:** Pachara Pholnak, Palakorn Boonsai, Autthaphol Theppaya, Yaowarat Sirisathitkul, Chitnarong Sirisathitkul

Manuscript number: **PCCC-2506-1402**

To appear in: Progresss in Color, Colorants and Coatings

Received: 10 June 2025

Final Revised: 18 August 2025

Accepted: 20 August 2025

Please cite this article as:

P. Pholnak, P. Boonsai, A. Theppaya, Y. Sirisathitkul, C. Sirisathitkul, Enhancing Anti-Aging Properties of Golden-Phase Leaves via Zinc Oxide–PVA–Chitosan Coating. Color, Colorants, Coat., 19 (2026) XX-XXX.

DOI: 10.30509/pccc.2025.167567.1402

This is a PDF file of the unedited manuscript that has been accepted for publication. The manuscript will undergo copyediting, typesetting, and review of the resulting proof before it is published in its final form

**Enhancing Anti-Aging Properties of Golden-Phase Leaves via Zinc Oxide–PVA–  
Chitosan Coating**

Pachara Pholnak<sup>1</sup>, Palakorn Boonsai<sup>1</sup>, Autthaphol Theppaya<sup>2</sup>, Yaowarat Sirisathitkul<sup>3,4\*</sup>,

Chitnarong Sirisathitkul<sup>4,5</sup>

<sup>1</sup> Department of Physical Science, Faculty of Science and Digital Innovation, Thaksin  
University (Phatthalung Campus), Phatthalung, Thailand

<sup>2</sup> Department of Design Art, Faculty of Fine and Applied Arts, Thaksin University,  
Songkhla, Thailand

<sup>3</sup> School of Engineering and Technology, Walailak University, Nakhon Si Thammarat,  
Thailand

<sup>4</sup> Functional Materials and Nanotechnology Center of Excellence, Walailak University,  
Nakhon Si Thammarat, Thailand

<sup>5</sup> Division of Physics, School of Science, Walailak University, Nakhon Si Thammarat,  
Thailand

\*Corresponding author: syaowara@mail.wu.ac.th

**Abstract**

The golden leaf vine (*Bauhinia aureifolia* K. & S.S. Larsen) is renowned for its distinct heart-shaped leaves and intricate vein patterns, which display natural variations in golden or reddish-brown hues. These unique leaves are traditionally used for decorative purposes and as components of handicraft items. This study aimed to enhance the durability and preserve the natural appearance of these golden-phase leaves with a protective coating. A composite of zinc oxide (ZnO) nanoparticles integrated with chitosan and polyvinyl

alcohol (PVA) was formulated and applied by spraying. The results demonstrated that the ZnO–PVA–chitosan composite effectively protected the leaves from moisture and ultraviolet (UV) radiation, significantly minimizing surface degradation and color fading after 18 cycles of accelerated aging. All RGB and CIELAB color indices showed less than **five** units of deviation from their initial values, indicating strong color retention. The increased L\* value reflected a brighter appearance in the spray-coated leaves. In addition to preserving color vibrancy, the composite coating also maintained the structural integrity of the leaves more effectively than the uncoated or differently coated samples. This spray coating of ZnO–PVA–chitosan offers a promising solution for extending the lifespan of golden-phase leaves used in cultural and decorative applications while preserving their natural beauty.

**Keywords:** Golden leaf vine; anti-aging coating; UV protection; zinc oxide; chitosan; polyvinyl alcohol

## 1. Introduction

*Bauhinia aureifolia* K. & S.S. Larsen, commonly known as the golden leaf vine, is a large woody climber native to the southern border provinces of Thailand, particularly in Narathiwat, Pattani, and Yala [1]. It thrives in rainforest environments, such as the Hala-Bala Wildlife Sanctuary and Bacho Waterfall National Park. This species is notable for its velvety, heart-shaped leaves that change color over time—from copper in the early stages, to brown, gold, and eventually silver before senescence [2]. The golden coloration becomes most vivid in mature plants over five years old, typically during June and July. Due to its striking appearance and textural qualities, this golden-phase leaf is of growing

interest for decorative and sustainable material applications [3]. However, only a limited number of harvested leaves are suitable for commercial use, and their aesthetic qualities are susceptible to deterioration influenced by environmental factors, age, and storage conditions. In response to community demand, recent efforts have focused on extending their lifespan in commercial utilization.

To address these preservation challenges, researchers have increasingly turned to innovative surface coatings—particularly those utilizing nanomaterials like zinc oxide (ZnO)—as a means to protect and prolong the visual and structural integrity of the golden leaves. Multifunctional ZnO has been applied to a variety of substrates, including textiles and other porous surfaces [4, 5]. Incorporating ZnO nanoparticles enhances the UV protection of polymers. For instance, ZnO-filled polystyrene exhibits ultraviolet (UV) absorption characteristics comparable to those of titanium dioxide and superior to those of nickel oxide and magnesium oxide [6]. When combined with chitosan, ZnO forms a versatile nanocomposite coating with promising applications across various fields [7, 8]. Metal nanoparticles have also been incorporated into chitosan to enhance adhesion, antimicrobial activity, and surface wettability of materials such as textiles and packaging films [9]. Similarly, ZnO–chitosan coatings demonstrate significantly stronger antimicrobial properties than chitosan alone. For instance, polyethylene films coated with ZnO–chitosan nanocomposites completely inactivated food pathogens, whereas chitosan-coated films only reduced viable cell counts by tenfold [10]. ZnO–chitosan coatings have demonstrated effectiveness against a wide range of bacteria, including both Gram-negative and Gram-positive strains. The incorporation of ZnO nanoparticles enhances the antibacterial activity by disrupting bacterial cell membranes and interfering with protein

synthesis [11, 12]. The amount of chitosan used during synthesis influences both the crystallite size and BET surface area of ZnO [13]. A larger quantity of chitosan leads to the formation of larger ZnO crystallites, which exhibit stronger UV absorbance across a broader wavelength range. However, ZnO with smaller crystallite sizes—formed with less chitosan—was more effective in inhibiting *Aspergillus* sp. growth on tube sedge basketry, likely due to its higher surface area and enhanced antimicrobial activity [13]. Adding ZnO nanoparticles to chitosan increases the solubility of the coating and enhances its thermal stability. The water contact angle also increases, indicating enhanced hydrophobicity. This property is desirable for a range of non-wettable surfaces, including plastics, fabrics, and paper [10, 14, 15]. ZnO–chitosan coatings also exhibit excellent barrier properties, reducing permeability and enhancing the protective effects against environmental factors [16, 17].

Composite coatings with ZnO are highly effective for food packaging applications, where they help reduce microbial and fungal growth. By minimizing microbial contamination, these coatings preserve the integrity of packaging materials and significantly extend the shelf life of food products [10, 18]. For example, ZnO has been combined with iron oxide and anthocyanins to develop a polyvinyl alcohol (PVA)-based smart packaging film for monitoring tomato freshness [19]. Similarly, ZnO-chitosan-coated films have been shown to significantly reduce bacterial and fungal loads in okra samples, demonstrating their potential for prolonging the shelf life of fresh vegetables [19]. The coatings have also been successfully applied to preserve the quality of various meat products, including fish balls, where they enhanced gas permeability and antibacterial effects [20]. Protective ZnO–chitosan coatings are also used to prevent metal

corrosion. The coatings can be impregnated with corrosion inhibitors, significantly enhancing their protective properties and reducing the amount of inhibitor needed [21, 22]. Furthermore, due to their biocompatibility and antimicrobial properties, ZnO–chitosan coatings are promising for biomedical applications, such as wound dressings and dental varnishes [23, 24]. They provide effective inhibition of bacterial growth and are suitable for use in medical devices [25, 26].

This study aims to enhance the utilization and durability of golden-phase leaves in decorations and handicrafts via antimicrobial and anti-aging ZnO–chitosan coatings, thereby adding commercial value to indigenous plants. However, applying protective coatings to natural substrates like dried leaves presents a unique challenge due to their irregular surface morphology, porosity, and fragility. Achieving uniform coverage and strong adhesion without compromising the aesthetic and structural integrity of the leaves requires carefully optimized formulations and gentle application techniques. PVA, a water-soluble and film-forming polymer, is incorporated in some formulations for its excellent mechanical strength and optical clarity. When blended with ZnO or chitosan, PVA improves nanoparticle dispersion and coating adhesion [27]. Depending on the composition, PVA can also modulate the viscosity of the solution, reducing aggregation and enhancing sprayability. In this work, ZnO–chitosan was coated by paint-brushing to promote uniform application on more viscous mixtures, while the less viscous ZnO–PVA and ZnO–PVA–chitosan formulations were applied by spraying. The results on moisture and UV resistance tests under accelerated aging conditions in a QUV chamber suggest that the optimum coating formulation and method provides the most effective protection in preserving the color and extending the shelf life of golden-phase leaves.

## 2. Experimental

### 2.1. Preparation of ZnO–chitosan, ZnO–PVA, and ZnO–PVA–chitosan coating solutions

To prepare the ZnO–chitosan coating solution for Sample B, an initial dissolution of 1.25 g of food-grade chitosan (Chitosan, L.B. Science; Mw. ~400) was conducted in 100 mL of 1% (v/v) acetic acid. This process was facilitated using a magnetic stirrer set at 300 rpm and proceeded for 2 hours until a clear and homogeneous solution was achieved. Subsequently, 5.00 g of commercial-grade ZnO nanopowder (MBK Chemical) was dispersed into 100 mL of 1% acetic acid, resulting in a preliminary suspension. The ZnO suspension was then methodically introduced into the chitosan solution by dropwise addition to avert nanoparticle agglomeration and foster uniform dispersion. After the integration, continuous stirring was executed with a high-speed homogenizer for an additional 2 hours to ensure the generation of a stable, moderately viscous solution devoid of gelation or particle aggregation. Their optical properties were measured in the wavelength range of 220–800 nm by the UV-Vis spectrophotometer (Shimadzu UV-2450).

In the synthesis of the ZnO–PVA coating solution for Sample C, a 1% (v/v) dilute acetic acid solution was formulated by incrementally introducing 1 mL of glacial acetic acid into 99 mL of deionized water, maintaining continuous agitation with a glass rod to achieve a uniform solution. Subsequently, a PVA solution was prepared at weight-to-volume ratios of 0.25:100 and 0.5:100 (PVA: deionized water, w/v). This mixture was agitated at 75°C using a magnetic stirrer until the PVA was fully solubilized, which generally required approximately 30 minutes. Concurrently, ZnO nanopowder was

measured at 0.25 g and 0.10 g, and each batch was cautiously dispersed into 100 mL of the pre-prepared 1% acetic acid solution under gentle stirring to ensure uniform dispersion. The resultant ZnO suspensions were subsequently introduced into the PVA solutions, followed by continuous agitation at a low speed for 1 hour to facilitate thorough mixing. This was followed by subjecting the coating solution to an ultrasonic bath for 1 hour at ambient temperature to augment nanoparticle dispersion and stability.

The ZnO–PVA–chitosan coating solution for Sample D was systematically synthesized via a sequential mixing procedure. Initially, a 1% (v/v) acetic acid solution was prepared by gradually introducing 1 mL of glacial acetic acid into 99 mL of deionized water under continuous agitation with a glass rod until complete homogenization was achieved. In a separate process, a PVA solution was prepared at a weight-to-volume ratio of 1:100 (PVA: deionized water, w/v), with stirring facilitated by a hotplate stirrer at 75°C for approximately 30 minutes until full polymer dissolution was attained. Simultaneously, 0.25 g of ZnO nanopowder was incrementally dispersed into 100 mL of the previously prepared 1% acetic acid solution, under gentle stirring to ensure uniform dispersion. Subsequently, the ZnO suspension was combined with 100 mL of the chitosan solution and the previously prepared PVA solution. This mixture was consistently stirred at a moderate speed using a hotplate stirrer for 30 minutes to promote a homogenous mixture of all components. Thereafter, the resultant coating solution underwent ultrasonication for 30 minutes at room temperature to augment nanoparticle dispersion and prevent agglomeration.

All prepared solutions were reserved for coating the surface of dried golden-phase leaves by either brushing (Sample B) or spraying (Samples C and D), depending on the



formulation, as part of an experimental study on maintaining their appearance and extending their lifespan by enhancing their resistance to moisture and ultraviolet degradation. Sample A, which was also used as the uncoated control, was compared with other coated samples. They were transferred into a tightly sealed container to mitigate air exposure and were stored under ambient conditions on a laboratory shelf.

**Table 1:** Formula and methods for coatings in this study.

| Sample No. | Chitosan (g) | Precursors |                     |         | Method of coating |
|------------|--------------|------------|---------------------|---------|-------------------|
|            |              | ZnO (g)    | 1% Acetic Acid (ml) | PVA (g) |                   |
| A          | -            | -          | -                   | -       | No Coating        |
| B          | 1.25         | 5.00       | 200                 | -       | Brush             |
| C          | -            | 0.25       | 100                 | 0.25    | Spray             |
| D          | 1.25         | 0.125      | 200                 | 1.00    | Spray             |

## 2.2. Preparation and coating of golden-phase leaves

Golden-phase leaves of the golden leaf vine were collected from two sources in Narathiwat Province—the Golden Leaf Group in Muang and Ra-Ngae Districts—and the Ban Bai Mai Group in Raman District, Yala Province. The fresh weight of the collected leaves ranged from 0.72 to 2.53 g. To dry the leaves, samples were placed in a plant press panel at ambient temperature (30–32°C) for one month. After drying, the golden-phase leaves were photographed and measured. Their dry weights ranged from 0.61 to 1.89 g, corresponding to a moisture content of 10.26–30.09%. The dried leaf samples were coated with four different coating formulations and methods, as summarized in Table 1, i.e., Sample A: uncoated control, Sample B: coated with ZnO–chitosan by brush painting,

Sample C: coated with ZnO–PVA by spraying, and Sample D: coated with ZnO–PVA–chitosan by spraying. For Samples B, C, and D, only the right half of each leaf was coated, leaving the left half uncoated for direct comparison.

### 2.3. Accelerated ageing test and characterization of coated leaves

Anti-aging of golden leaves was tested using a QUV accelerator (Model QUV/spray, Q-Lab Corporation, distributed by Color Global Co., Ltd.), an extensively employed apparatus for the simulation of environmental degradation in materials. This device possesses the capability to replicate outdoor weathering conditions—such as UV radiation, moisture, and condensation—within a considerably reduced timeframe. Whereas exposure in natural settings may span several months or years, QUV testing can produce analogous degradation effects in merely a few weeks. The degradation study was conducted in compliance with ASTM D4799/D4799M-17 standards. Specimens were systematically placed within the QUV chamber and exposed to cyclic environmental conditions. Each cycle entailed UV-A irradiation at a wavelength of 340 nm, maintained at a consistent temperature of 50°C for 4 hours, followed by a 15-minute water spray interval. Subsequently, the samples underwent a condensation phase at 50°C for 8 hours. Therefore, one complete cycle constituted a 12-hour duration, consisting of 4 hours of UV exposure and 8 hours of moisture condensation under meticulously controlled thermal conditions. After 1, 2, 4, 10, 14, and 18 cycles, the surface color and visual characteristics of the specimens were scrutinized to assess the extent of degradation. Microscopic surface morphology and elemental composition of Sample D after 18 cycles of accelerated ageing were also analyzed using Scanning Electron Microscopy (SEM)

coupled with Energy Dispersive Spectroscopy (EDS).

Color test results of accelerated golden leaves were obtained using the Colorimetry technique with a Spectrophotometer (CM-5, Konica Minolta). The CM-5 Spectrophotometer by Konica Minolta is a bench-top measurement instrument designed for color analysis of opaque, transparent, and translucent samples. It is widely used in research and laboratory environments to evaluate color and appearance in various materials, including solids, liquids, pastes, powders, pills, and granules. Leaf samples were placed on the top-port measurement area after calibration of the device. In the measurement process, the reflectance mode was selected, and the MEAS button was pressed to capture the color data. The device displayed both RGB and CIELAB color indices, spectral curves, and color difference graphs. However, all color difference calculations ( $\Delta E$ ) were based on the CIELAB system, as it provides a perceptually uniform metric [28]. The  $\Delta E$  values were calculated using the standard formula:

$$\Delta E = \sqrt{(L_1 - L_2)^2 + (a_1 - a_2)^2 + (b_1 - b_2)^2} \quad (1)$$

where L, a, and b represent the lightness and chromaticity coordinate before and after accelerated aging, respectively.





### 3. Results and Discussion

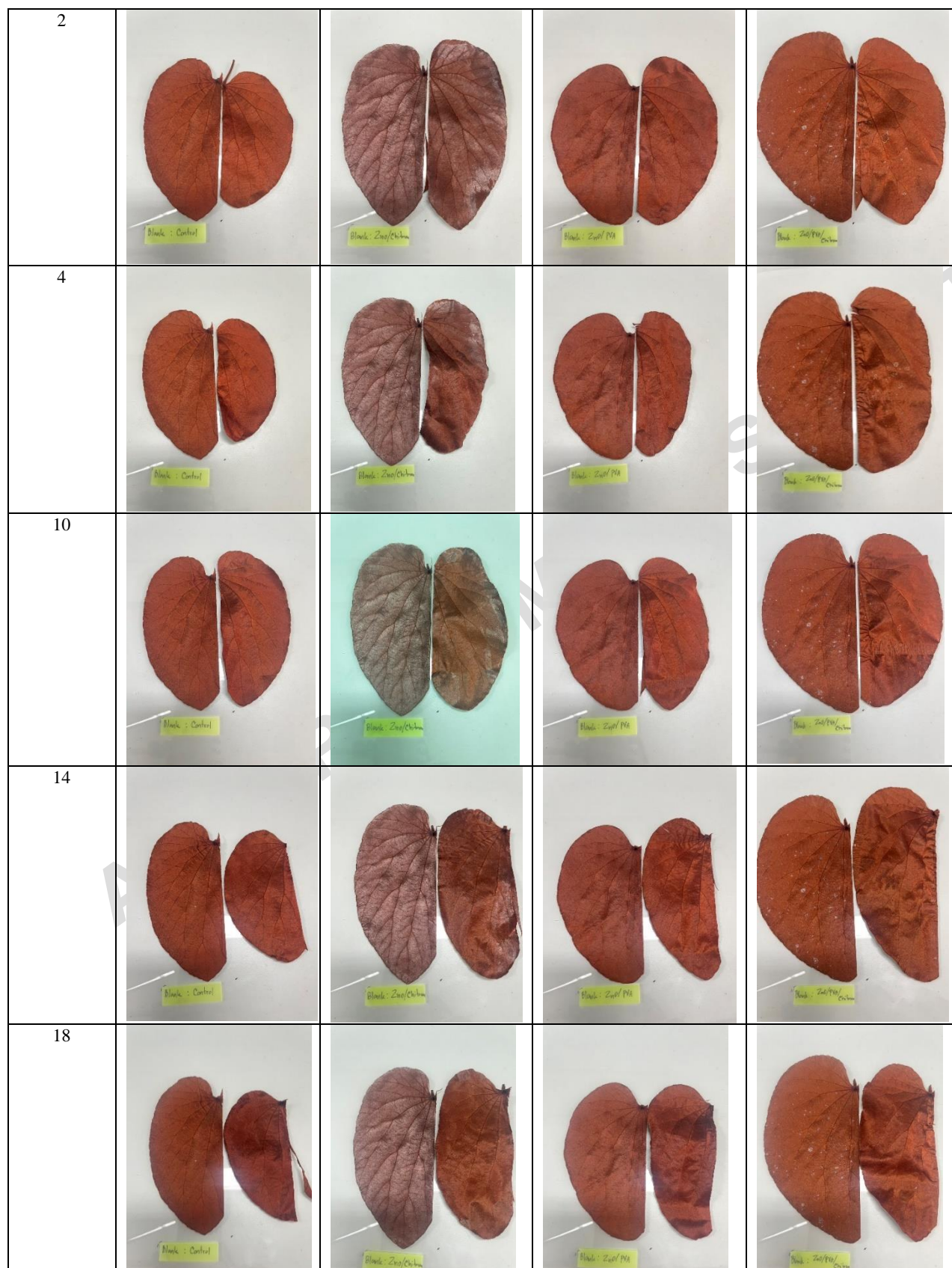
#### 3.1. Physical characteristics

Figure 1a exemplifies the front and back views of four golden-phase leaves. Separately, Figure 1b illustrates uncoated dried leaves—before the application of any coating material—that retained their original shape after a month in the plant press panel. These leaves remained intact and flexible, without brittleness or breakage, and their natural

golden color was preserved without **visible fading**. Table 2 shows the color and physical appearance of golden-phase leaves after undergoing accelerated aging tests at a temperature of 50°C for 12 hours per cycle. After the 4 hours of UV exposure followed by 8 hours of water mist exposure in the first cycle, all samples exhibited minor leaf wrinkling. With increasing cycles, the uncoated sample A showed noticeable color fading, and the leaf edges were wrinkled and curled, similar to the **uncoated** left side of samples B–D. The right side of Sample B, coated with a ZnO–chitosan by paint brushing, has a darker color with signs of tearing on the leaf surface and wrinkled, torn edges. Sample C, coated with a ZnO–PVA by spraying on the right side, showed only slight color fading and no edge wrinkling. Similarly, Sample D, coated with a ZnO–PVA–chitosan by spraying on the right side, also showed only slight fading and no wrinkling at the leaf edges, consistent with the results observed in Sample C.

**Table 2:** Images of golden leaves tested with an accelerator up to 18 cycles.

| Number of Cycles | Samples   |   |  |   |
|------------------|---|---|--|---|
|                  | A<br>Control<br>No Coating  | B<br>ZnO–chitosan<br>Coating  | C<br>ZnO–PVA<br>Coating  | D<br>ZnO–PVA–chitosan<br>coating  |
| 1                |  |  |  |  |





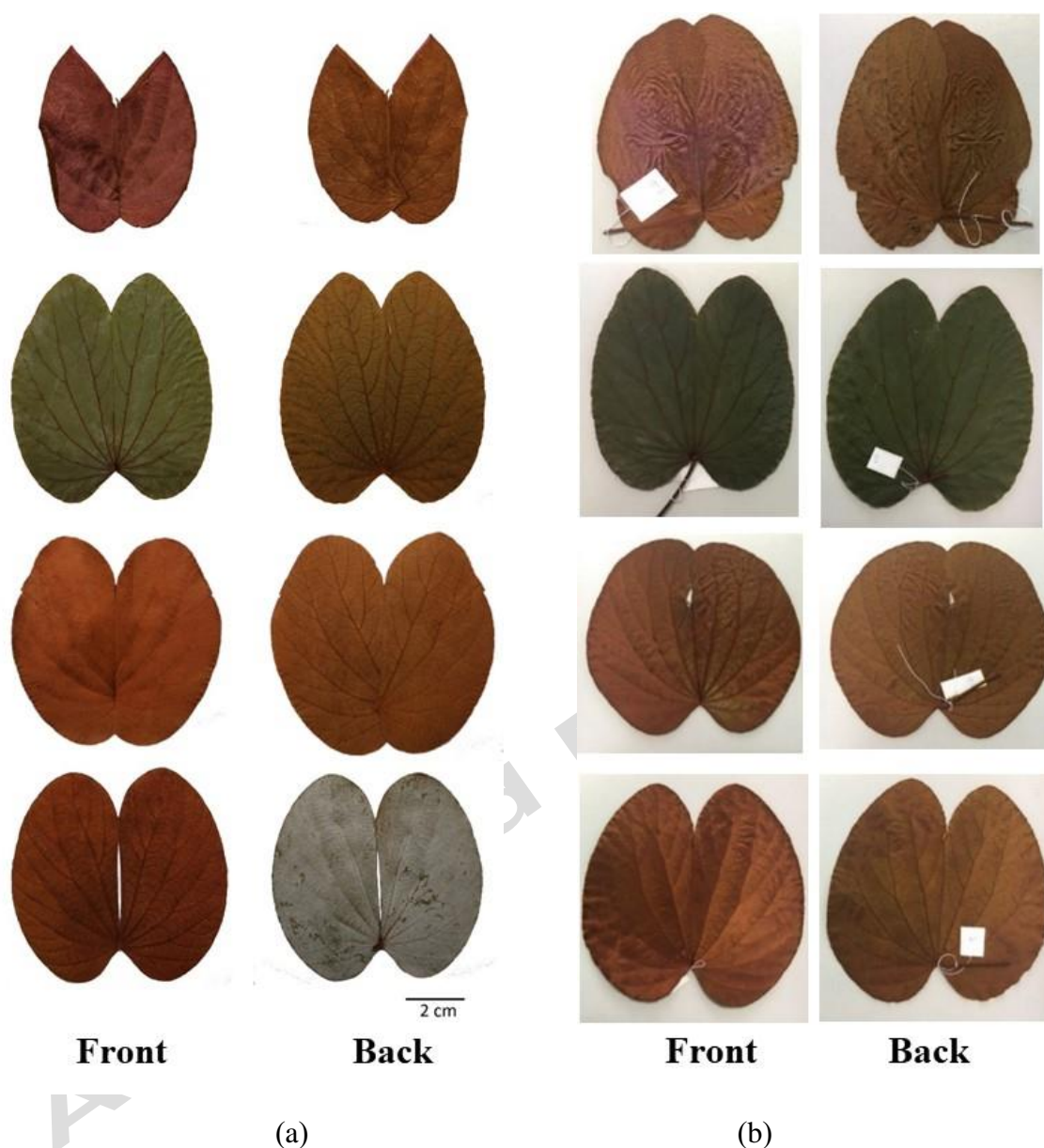


**Figure 1:** Examples of color variations in (a) fresh golden-phase leaves and (b) dried leaves after a month in the plant press panel.

### 3.2. Microscopic and UV-vis studies

Figure 2 compares SEM images of coated surfaces alongside a control sample after 18 cycles of accelerated aging. In the uncoated sample A18 (Figure 2a), micropits are uniformly distributed across the surface. For the brushed layer of sample B18 (Figure

2b), ZnO nanoparticles are evenly dispersed within the rough binder matrix, with particle sizes ranging from approximately 100 to 1600 nm. In samples C18 (Figure 2c) and D18 (Figure 2d), thin plate-like nanoparticles have aggregated into larger clusters. This clustering likely results from increased electrostatic forces between the nanoparticles during the spraying process, which brings them into closer proximity and facilitates aggregation. These relatively large ZnO clusters are likely advantageous in UV absorption [13]. The UV absorption characteristics of the coatings were confirmed by the UV-vis spectra shown in Figure 3a. A broad absorption band was observed with a pronounced peak occurring between approximately 220 and 400 nm. This range corresponds to the UV region, indicating that the ZnO-chitosan coatings are highly effective in absorbing UV radiation. The strong absorption in this region is primarily attributed to the wide bandgap of ZnO nanoparticles, which enables them to block harmful UV rays and contribute to the photostability of the coated golden-phase leaves. In Figure 3b, the EDS spectrum of sample D18 shows that the regions where the coating adheres contain Zn and oxygen (O) as the primary elements. Interestingly, previous studies have demonstrated the absorption of Zn by plants through ZnO nanoparticle coatings [29, 30].

Additionally, potassium is detected because it is a natural component of plant leaves. Other detected trace elements are likely due to impurities in the chitosan. The carbon signal is attributed to the carbon tape used to mount the samples, while the silicon signal originates from the glass substrate.

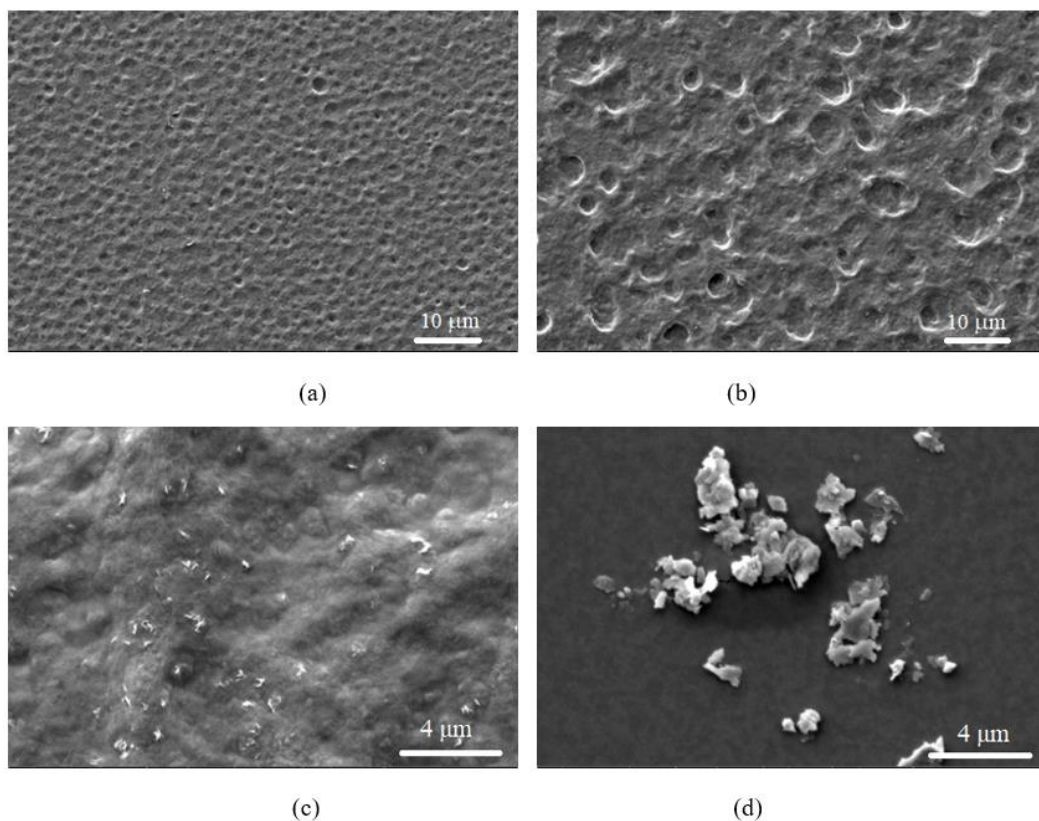


**Figure 2:** SEM micrographs of samples (a) A18, (b) B18, (c) C18, and (d) D18.

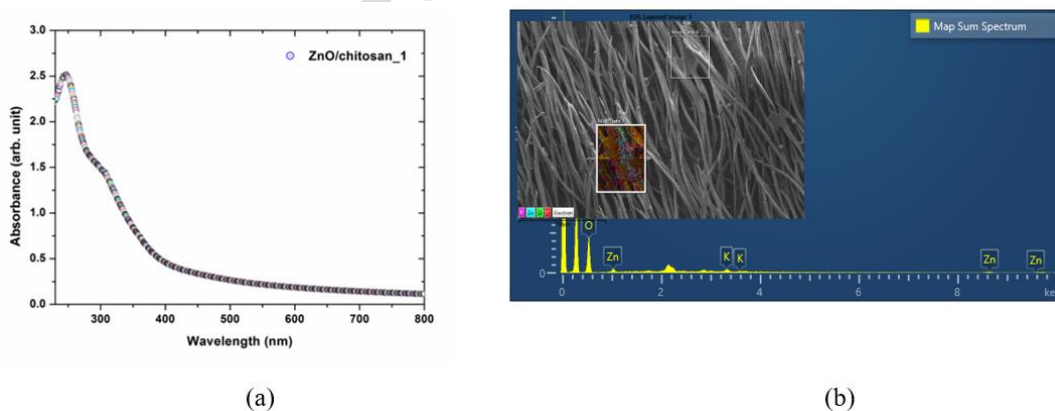


**Figure 3:** Examples of (a) UV-vis and (b) elemental spectra.

### 3.3. Color changes

Table 3 compares the color indices of golden-phase leaves across different cycles of QUV accelerated aging. Without coating (samples A1–A18), the R and G color indices are significantly reduced, while the B index tends to increase, as the number of **aging**



**cycles increases.** For the coated samples, the colors change progressively with increased cycles of accelerated aging. These color changes are due to prolonged exposure to humidity from water mist during testing, which may have caused the PVA and chitosan binders to degrade and detach from the leaf surface. Furthermore, repeated and extended exposure to UV **light has** directly impacted the surface areas exposed to the radiation, contributing to the color fading. Decreases in the  $a^*$  (red-green) and  $b^*$  (yellow-blue) values suggest a gradual loss of vibrancy.

**Table 3** Comparison of RGB and CIELAB colors of golden-phase leaves after up to 18 cycles of accelerated aging test.

| Samples | Coating Formulation | Method | QUV Cycles | RGB |    |    | CIELAB |       |       |                        |
|---------|---------------------|--------|------------|-----|----|----|--------|-------|-------|------------------------|
|         |                     |        |            | R   | G  | B  | $L^*$  | $a^*$ | $b^*$ | $\Delta E_{L^*a^*b^*}$ |
| A0      | Uncoated            | -      | 0          | 102 | 45 | 24 | 26.34  | 20.21 | 20.52 | -                      |
| A1      | Uncoated            | -      | 1          | 101 | 43 | 24 | 25.68  | 20.68 | 19.98 | 0.9737                 |
| A2      | Uncoated            | -      | 2          | 102 | 42 | 24 | 25.76  | 21.38 | 20.09 | 1.375                  |
| A4      | Uncoated            | -      | 4          | 101 | 40 | 24 | 25.15  | 21.62 | 19.29 | 2.218                  |
| A10     | Uncoated            | -      | 10         | 102 | 46 | 28 | 26.61  | 19.73 | 18.85 | 1.759                  |
| A14     | Uncoated            | -      | 14         | 100 | 42 | 27 | 25.49  | 20.60 | 18.44 | 2.281                  |
| A18     | Uncoated            | -      | 18         | 96  | 39 | 27 | 24.08  | 20.67 | 17.07 | 4.150                  |
| B0      | ZnO-chitosan        | Brush  | 0          | 83  | 52 | 46 | 25.50  | 10.72 | 7.71  | -                      |
| B1      | ZnO-chitosan        | Brush  | 1          | 90  | 49 | 38 | 25.55  | 14.42 | 12.41 | 5.982                  |
| B2      | ZnO-chitosan        | Brush  | 2          | 93  | 54 | 43 | 27.33  | 13.40 | 11.83 | 5.245                  |
| B4      | ZnO-chitosan        | Brush  | 4          | 91  | 51 | 41 | 26.25  | 13.99 | 11.81 | 5.298                  |
| B10     | ZnO-chitosan        | Brush  | 10         | 97  | 51 | 36 | 27.08  | 15.97 | 15.38 | 9.428                  |
| B14     | ZnO-chitosan        | Brush  | 14         | 95  | 49 | 35 | 26.31  | 16.25 | 15.11 | 9.274                  |
| B18     | ZnO-chitosan        | Brush  | 18         | 102 | 50 | 31 | 27.66  | 17.86 | 18.34 | 12.99                  |

|     |                      |       |    |     |    |    |       |       |       |        |
|-----|----------------------|-------|----|-----|----|----|-------|-------|-------|--------|
| C0  | ZnO–PVA              | Spray | 0  | 97  | 48 | 33 | 26.39 | 17.09 | 15.77 | -      |
| C1  | ZnO–PVA              | Spray | 1  | 101 | 42 | 26 | 25.55 | 21.04 | 18.70 | 4.989  |
| C2  | ZnO–PVA              | Spray | 2  | 93  | 54 | 43 | 27.33 | 13.40 | 11.83 | 5.479  |
| C4  | ZnO–PVA              | Spray | 4  | 100 | 45 | 29 | 26.04 | 19.77 | 17.77 | 3.362  |
| C10 | ZnO–PVA              | Spray | 10 | 104 | 43 | 25 | 26.37 | 21.29 | 20.04 | 5.989  |
| C14 | ZnO–PVA              | Spray | 14 | 102 | 42 | 26 | 25.83 | 21.23 | 19.33 | 5.489  |
| C18 | ZnO–PVA              | Spray | 18 | 93  | 42 | 31 | 24.10 | 18.48 | 14.81 | 2.846  |
| D0  | ZnO–PVA–<br>chitosan | Spray | 0  | 97  | 45 | 28 | 25.76 | 18.40 | 18.01 | -      |
| D1  | ZnO–PVA–<br>chitosan | Spray | 1  | 97  | 44 | 27 | 25.31 | 19.09 | 18.06 | 0.825  |
| D2  | ZnO–PVA–<br>chitosan | Spray | 2  | 107 | 51 | 29 | 28.64 | 19.56 | 20.23 | 3.817  |
| D4  | ZnO–PVA–<br>chitosan | Spray | 4  | 103 | 51 | 30 | 27.91 | 17.94 | 19.10 | 2.454  |
| D10 | ZnO–PVA–<br>chitosan | Spray | 10 | 98  | 45 | 26 | 25.74 | 18.95 | 19.11 | 1.230  |
| D14 | ZnO–PVA–<br>chitosan | Spray | 14 | 99  | 47 | 29 | 26.53 | 18.26 | 18.29 | 0.8312 |
| D18 | ZnO–PVA–<br>chitosan | Spray | 18 | 101 | 46 | 29 | 26.45 | 19.35 | 18.02 | 1.174  |

Comparing color changes after 18 cycles of accelerated aging in Figure 4, samples with ZnO–PVA spray-coating show smaller changes in RGB and L\*a\*b\* color indices, maintaining a closer resemblance to their initial state (sample C0) even after 18 cycles of accelerated aging (sample C18). Among all samples, sample D18 with ZnO–PVA–chitosan coating maintains a color appearance closest to the initial state (sample D0) with only slight fading observed after 1–18 cycles of accelerated aging. Following 18 cycles, all color indices of the leaf surface show only minimal increases. Notably, sample

D18 appears slightly brighter, as indicated by the rise in the  $L^*$  index, whereas sample C18 and the uncoated control sample A18 exhibit a darker appearance.

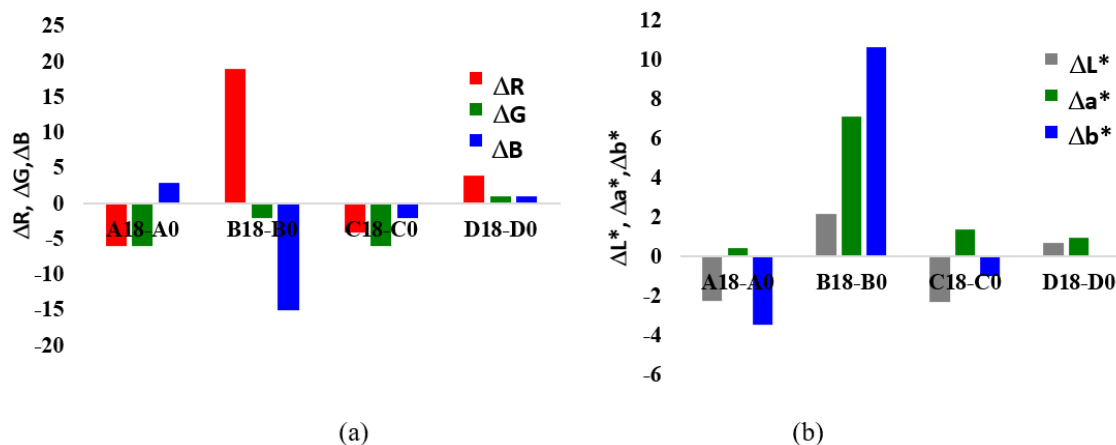


**Figure 4:** Changes in (a) RGB and (b)  $L^*a^*b^*$  color indices of the golden leaves after the QUV acceleration for 18 cycles (comparing Samples A18, B18, C18, and D18 to A0, B0, C0, and D0).

Table 3 also presents the color differences ( $\Delta E$ ) compared to the initial state of the samples. Among all samples, those coated with ZnO–chitosan by brush application (samples B1–B18) exhibited the most pronounced color variation. This is likely due to the brushed-on coating being less resistant to prolonged exposure to moisture from steam and water droplets during repeated accelerated aging cycles, leading to partial detachment from the leaf surface. Across all sample sets, some fluctuations in  $\Delta E$  values were observed between cycles. These inconsistencies may be attributed to minor measurement uncertainties, possibly arising from differences in sample positioning or surface conditions during each reading. In agreement with the findings shown in Figure 4, the ZnO–PVA–chitosan coated samples demonstrated the smallest color changes, with  $\Delta E$  values ranging from 0.823 to 3.817. This indicates strong resistance to fading and

suggests that the ZnO–PVA–chitosan formulation offers the most effective protection for preserving the original appearance of golden-phase leaves, outperforming both other coating types and the uncoated control. To further expand the functional potential of this composite coating, future research will explore its antimicrobial efficacy [24] and self-cleaning properties [31], thereby reinforcing its suitability for sustainable decorative and preservation applications.

#### 4. Conclusions

The golden-phase leaves of *B. aureifolia* K. & S.S. Larsen retained their original shape, color, and flexibility after drying for one month, without signs of brittleness or discoloration (e.g., browning). Under accelerated aging conditions, progressive color fading was observed with increasing cycles. Extended exposure to UV light over multiple cycles led to additional fading, especially in areas directly exposed to UV radiation. Among the three coatings evaluated, the golden-phase leaves coated with the ZnO–PVA–chitosan demonstrated superior protection against moisture and UV radiation, showing only minimal fading even after 18 aging cycles, while maintaining a color closest to the initial stage. When applied via spraying, this coating adhered uniformly to the leaf surface, effectively enhancing the durability of the golden-phase leaves. From an application perspective, the ZnO–PVA–chitosan spraying offers promising protection against both moisture and UV exposure, contributing to the preservation of appearance and the extended lifespan of local handicraft items and decorative products made from golden-phase leaves.

## 5. References

1. Sraphet S, Sukawutthiya P, Srisawad N, Duncan RS, Triwitayakorn K. Evaluation of the genetic diversity of *Bauhinia winitii*, an endemic plant of Thailand, using microsatellite markers. *Philipp J Sci.* 2021; 150(2):557–569. <https://doi.org/10.56899/150.02.20>
2. Larsen K, Larsen SS. Notes on the genus *Bauhinia* (Leguminosae-Caesalpinioideae) in SE Asia. *Nord J Bot.* 1991; 11(6):629–634. <https://doi.org/10.1111/j.1756-1051.1991.tb01275.x>
3. Theppaya A, Ruttajorn K. The design and development of golden leaf products to enhance marketing value in southernmost provinces. *Parichart J.* 2024; 37(4):828–843. <https://doi.org/10.55164/pactj.v37i4.272381>
4. Kora AJ. Leaves as dining plates, food wraps and food packing material: Importance of renewable resources in Indian culture. *Bull Natl Res Cent.* 2019; 43:205. <https://doi.org/10.1186/s42269-019-0231-6>
5. Elsamanoudy G, Mahmoud NSA, Alexiou P. Handwoven interior accessories from palm leaves as sustainable elements. *J Cult Heritage Manage Sust Dev.* 2024; online first. <https://doi.org/10.1108/JCHMSD-05-2023-0054>
6. Pardi H, Fitriyah D, Silitonga FS, Edelwis TW, Wardani RK, Permana D, Priyanga A, Fitriyah D, Ramdhani EP. The antimicrobial potential of ZnO-chitosan/pandan leaves: Advancing antimicrobial textile technology. *J Dispers Sci Technol.* 2025; 46(4):601-610. <https://doi.org/10.1080/01932691.2023.2296593>

7. Zare A. Application of  $\beta$ -CD to control the release of ZnO nanoparticles on the silk fabric surface along with citric acid as eco-friendly cross-linker. *Prog Color Colorant Coat.* 2023;16(3):295-307. <https://doi.org/10.30509/pccc.2023.167048.1193>
8. AL-Rubaiawi HK, Faisal Alwan A, Ayad Husain A, Muhamed Ibrahim N, Abdul Kareem Ali D, Tariq Mahmood A. Structural and optical properties of doped polystyrene thin films by (NiO, TiO<sub>2</sub>, ZnO, MgO) nanoparticles. *Prog Color Colorant Coat.* 2025;18(3):323-341. <https://doi.org/10.30509/pccc.2025.167428.1344>
9. Dejene BK, Abtew MA. Chitosan/zinc oxide (ZnO) nanocomposites: A critical review of emerging multifunctional applications in food preservation and biomedical systems. *Int J Biol. Macromol.* 2025; 316(1):144773. <https://doi.org/10.1016/j.ijbiomac.2025.144773>
10. Chavez-Esquivel G, Ángeles-Beltrán D, Tellez de la Torre PM, Cortes-Cordova DE, Huerta-Arcos L, Estrada de los Santos P. Antimicrobial and antifungal edible coatings with ZnO nanoparticles dispersed in a chitosan-guar gum matrix for hass avocado preservation. *Int J Biol Macromol.* 2025; 308(Part 4):142467. <https://doi.org/10.1016/j.ijbiomac.2025.142467>
11. Sadeghi-Kiakhani M, Hashemi E. Study on the effect of pomegranate peel and walnut green husk extracts on the antibacterial and dyeing properties of wool yarn treated by chitosan/Ag, chitosan/Cu nano-particles. *Prog Color Colorant Coat.* 2023; 16(3):221-229. <https://doi.org/10.30509/pccc.2022.167030.1188>
12. Al-Naamani L, Dobretsov S, Dutta J. Chitosan-zinc oxide nanoparticle composite coating for active food packaging applications. *Innov Food Sci Emerg Technol.* 2016; 38(A): 231-237. <https://doi.org/10.1016/j.ifset.2016.10.010>

13. Wei X, Li Q, Wu C, Sun T, Li X. Preparation, characterization and antibacterial mechanism of the chitosan coatings modified by Ag/ZnO microspheres. *J Sci Food Agric.* 2020; 100(15):5527-5538. <https://doi.org/10.1002/jsfa.10605>
14. Haldorai Y, Shim JJ. Chitosan-Zinc Oxide hybrid composite for enhanced dye degradation and antibacterial activity. *Compos Interfaces.* 2013; 20(5):365-377. <https://doi.org/10.1080/15685543.2013.806124>
15. Pholnak P, Khongbun J, Suksom K, Lertworapreecha M, Suwanboon S, Sirisathitkul C. Antifungal efficacy of chitosan-modified zinc oxide nanoparticles on tube sedge products. *J Nanostruct.* 2020; 10(2):424-433. <https://doi.org/10.22052/JNS.2020.02.020>
16. Yu D, Basumatary IB, Liu Y, Zhang X, Kumar S, Ye F, Dutta J. Chitosan-photocatalyst nanocomposite on polyethylene films as antimicrobial coating for food packaging. *Prog Org Coat.* 2024; 186:108069. <https://doi.org/10.1016/j.porgcoat.2023.108069>
17. Evren G, Koşak Söz Ç, Özomay Z, Uzun M, Sönmez S. Effect of the coating formulation on the barrier properties and final appearance of non-wettable hybrid paper sheets. *Prog Color Color Coat.* 2024; 17(3):239-262. <https://doi.org/10.30509/pccc.2024.167221.1257>
18. Márton P, Nagy ÖT, Kovács D, Szolnoki B, Madarász J, Nagy N, Szabó GS, Hórvölgyi Z. Barrier behaviour of partially N-acetylated chitosan layers in aqueous media. *Int J Biol Macromol.* 2023; 232:123336. <https://doi.org/10.1016/j.ijbiomac.2023.123336>

19. Szőke ÁF, Szabó G, Simó Z, Hórvölgyi Z, Albert E, Végh AG, Zimányi L, Muresan LM. Chitosan coatings ionically cross-linked with ammonium paratungstate as anticorrosive coatings for zinc. *Eur Polym J.* 2019; 118:205-212. <https://doi.org/10.1016/j.eurpolymj.2019.05.057>
20. Al-Naamani L, Dutta J, Dobretsov S. Nanocomposite zinc oxide-chitosan coatings on polyethylene films for extending storage life of okra (*Abelmoschus esculentus*). *Nanomater.* 2018; 8(7):479. <https://doi.org/10.3390/nano8070479>
21. Sathianathan RV, Joseph J, Ilanthendral K, Raveena R. Analysis of smart packaging film for tomato freshness: ZnO-Fe<sub>2</sub>O<sub>3</sub>/PVA with *Musa paradisiaca* bract anthocyanin. *Food Biophys.* 2025; 20:84. <https://doi.org/10.1007/s11483-025-09971-w>
22. Wei XQ, Li XP, Wu CL, Yi SM, Zhong KL, Sun T, Li JR. The modification of in situ SiO<sub>x</sub> chitosan coatings by ZnO/TiO<sub>2</sub> NPs and its preservation properties to silver carp fish balls. *J Food Sci.* 2018; 83(12):2992-3001. <https://doi.org/10.1111/1750-3841.14381>
23. Szőke ÁF, Szabó GS, Hórvölgyi Z, Albert E, Végh AG, Zimányi L, Muresan LM. Accumulation of 2-Acetylamino-5-mercapto-1,3,4-thiadiazole in chitosan coatings for improved anticorrosive effect on zinc. *Int J Biol Macromol.* 2020; 142:423-431. <https://doi.org/10.1016/j.ijbiomac.2019.09.114>
24. Szőke ÁF, Szabó GS, Hórvölgyi Z, Albert E, Gaina L, Muresan LM. Eco-friendly indigo carmine-loaded chitosan coatings for improved anti-corrosion protection of zinc substrates. *Carbohydr Polym.* 2019; 215:63-72. <https://doi.org/10.1016/j.carbpol.2019.03.077>



25. Wafi A, Khan MM. Green synthesized ZnO and ZnO-based composites for wound healing applications. *Bioprocess Biosyst Eng.* 2025; 48:521–542. <https://doi.org/10.1007/s00449-024-03123-z>
26. Monika P, Hari Krishna R, Hussain Z, Nandhini K, Pandurangi SJ, Malek T, Kumar SG. Antimicrobial hybrid coatings: A review on applications of nano ZnO based materials for biomedical applications, *Biomater Adv.* 2025; 172:214246. <https://doi.org/10.1016/j.bioadv.2025.214246>
27. Salama A. Chitosan/silk fibroin/zinc oxide nanocomposite as a sustainable and antimicrobial biomaterial. *Cellul Chem Technol.* 2018; 52(9-10):903-907
28. Harini B, Rajeshkumar S, Roy A. Biomedical application of chitosan and piper longum-assisted nano zinc oxide–based dental varnish. *Appl Biochem Biotechnol.* 2022;194(3):1303-1309. <https://doi.org/10.1007/s12010-021-03712-8>
29. Dejen KD, Zereffa EA, Murthy HCA, Merga A. Synthesis of ZnO and ZnO/PVA nanocomposite using aqueous Moringa Oleifera leaf extract template: Antibacterial and electrochemical activities. *Rev Adv Mater Sci.* 2020; 59(1):464-476. <https://doi.org/10.1515/rams-2020-0021>
30. Sirisathitkul Y, Kaewareelap S. Color analysis of batik fabric by facile smartphone colorimetry. *Int J Adv Sci Eng Inf Technol.* 2021; 11(1):84–91. <https://doi.org/10.18517/ijaseit.11.1.11480>
31. Read TL, Doolette CL, Li C, Schjoerring JK, Kopittke PM, Donner E, Lombi, E. Optimising the foliar uptake of zinc oxide nanoparticles: Do leaf surface properties and particle coating affect absorption?. *Physiol Plant.* 2020; 170:384-397. <https://doi.org/10.1111/ppl.13167>

32. Adhikari T, Kundu S, Rao AS. Zinc delivery to plants through seed coating with nano-zinc oxide particles. *J Plant Nutr.* 2016; 39(1):136–146.  
<https://doi.org/10.1080/01904167.2015.1087562>
33. Gabriela RN, Heryanto H, Tahir D. Nanocomposite  $\text{TiO}_2/\text{ZnO}$ /chitosan by method sol-gel for self-cleaning application. *Int J Biol Macromol.* 2025; 298:140076.  
<https://doi.org/10.1016/j.ijbiomac.2025.140076>